



## **DAMPING FACTORS AND EQUIVALENT SDOF DEFINITION IN THE DISPLACEMENT-BASED ASSESSMENT OF MONUMENTAL MASONRY STRUCTURES**

**Sonia RESEMINI<sup>1</sup>, Sergio LAGOMARSINO<sup>1</sup> and Sonia GIOVINAZZI<sup>1</sup>**

### **SUMMARY**

The recent Italian seismic decrees (OPCM 3274/2003 and OPCM 3431/2005) have strongly modified the safety concept for existing buildings. This code introduces the idea of design and verification through performance-based analysis. Unfortunately, in case of monumental heritage, the OPCM 3431 decree does not propose a specific methodology. For masonry historical structures, the available literature on this topic generally deals with the out-of-plane overturning mechanism, considering the wall as an oscillating rigid block (e.g., façades or bell towers). As a matter of fact, for these structures or macroelements, the fundamental periods are large, even for the initial elastic range, and they can increase because of cracking in masonry, typically considered as no-tension material. The effects of these features on the dynamic response and the related prediction of displacement capacity need to be investigated. For this purpose, non-linear dynamic analyses on the equivalent SDOF systems are performed, employing different input ground motions. These analyses may be useful to evaluate the influence of factors such as: 1) the feasibility of the equivalent SDOF system definition for the displacement-based procedure (as for mainly rocking system, the model is derived by Housner's non-linear oscillator, having elastic behaviour, with softening range); 2) the equivalent viscous damping relationship and the consequent displacement response spectrum reduction for the long-period range.

### **1. INTRODUCTION**

The assessment of the consequences to monumental buildings, after recent Italian seismic events (Umbria-Marche 1997, Piedmont, 2000-2003, Apulia and Molise, 2002, Lombardy 2004) has highlighted how, according to their architectonic complexity (geometry, constructive phases, transformations, etc.) and the poor tensile strength of the masonry, the damage and collapse often take place locally. Due to the dynamic action, the structure is subdivided into macroelements (Dogliani *et al.* 1994), which are characterized by a mostly autonomous structural behaviour on respect to the rest of the building. For the churches, representing the majority of the monumental heritage in Italy, the possibility of local failure is higher due to the presence of intrinsic vulnerability i.e. wide halls, long thin span vaults, slender towering or projecting parts, slender walls with large openings, different constructive phases, etc.

Observing the damage occurred in real cases, it was pointed out that, if the masonry shows good characteristics (regular texture, transversal connection between the leaves), the damage mechanisms develop as loss of equilibrium of rigid blocks capable of sliding and rotating.

From these considerations the use of the kinematic approach (Heyman 1966), based on the equilibrium limit analysis, has been adopted as a feasible criterion to check the safety of these local mechanisms. Actually the out-of-plane mechanisms, typically non-linear, show high displacement capacity until collapse. As a matter of fact since an earthquake is a dynamic action, the static loss of equilibrium does not correspond to the collapse, and the kinematism is able to sustain some horizontal action even after its activation.

---

<sup>1</sup> Department of Structural and Geotechnical Engineering, University of Genoa, Italy  
Reference email : resemmini@diseg.unige.it

OPCM 3431/2005 seismic code proposes, for existing buildings, a displacement-based method, where reference is made to the kinematic analysis for the assessment of the horizontal acceleration that activates the mechanism and for the assessment of the mechanism ultimate capacity in terms of horizontal displacement (non-linear approach).

Even though pointing out the need for a quantitative evaluation, OPCM 3431/2005 seismic code does not specify how to apply the displacement-based method in the case of monumental heritage. Theoretically, the safety check could be based on the same concepts and procedures, but various issues still need to be pointed out.

First of all, it is necessary to define an equivalent SDOF system representative of a plausible kinematic configuration of monumental buildings or their macroelements (e.g., façades or bell towers).

Secondly, the capacity curve obtained by the use of non-linear kinematic approach, disregards the deformability of the macroelement that is involved in the collapse mechanism, as it is considered made by rigid blocks. Hence, an estimate of the vibration period  $T_0$ , associated to the mechanism in the phase preceding its activation, is aimed. The definition of the initial period is a difficult task dealing with kinematism of macroelements as actually their initial dynamic behaviour is realistically related both to the element stiffness and to the structure stiffness, because of their interaction.

Finally, with regard to the representation of the seismic demand, some specific considerations are needed for the response spectra reduction in the particular case of monumental heritage. The use of inelastic spectra seems not be feasible for monumental buildings or their macroelements. In fact, peculiar monumental structures (bell-towers, churches, obelisks) and their macroelements have high fundamental period of vibration still in the elastic range. The period can further increase because of the nearly non-tensile strength of masonry causing widespread cracking ( $T > 2.5-4s$ ). Their ductility is therefore expected to be higher than the limit value for which the reduction factors, function of the ductility (Fayfar 2000), are defined and can be employed. Moreover, when inelastic spectra are employed, the resulting seismic demand in terms of displacement is strongly influenced by the definition of the initial period  $T_0$  that, as already stated, is difficult to be achieved for monumental structures and even more dealing with the analysis of single macroelement.

As a feasible alternative, the use elastic demand spectrum (5% damping) has been proposed (Lagomarsino 2005) for the assessment of the target displacement by an iterative procedure considering a properly defined equivalent secant stiffness. According to this method, the equivalent period  $T^*$ , useful for the evaluation of the target displacement  $S_d^*$ , has to be defined by a linear interpolation between two assumed period values corresponding to the initial and the collapse phase. However, there are some critical aspects affecting this proposal: a) the results in terms of displacement response is still affected by the initial period value  $T_0$ , b) the expected displacement is not well represented in the low-medium range of the non-linear phase.

In order to overcome the highlighted problems, a new proposal for a non-linear kinematic simplified approach is promoted, where overdamped elastic spectra are introduced in order to evaluate the maximum response in terms of displacement (or rotation  $\theta$ ) for macroelements belonging to monumental structures.

The implementation of the proposed models requires, as the previous one (Lagomarsino 2005), the definition of a substitute-structure model for the macroelements, of a representative non-linear elastic force-displacement relationship, to be obtained performing a non-linear kinematic analysis, and lastly the proposal of a representative damping relationship.

The main objectives of this paper are, first of all, the investigation of how a different definition of these features can affect the dynamic response of a substitute structure and secondly the investigation of the reliability of the displacement prediction by the newly proposed simplified approach.

For this purpose, systematic non-linear dynamic analyses on the equivalent SDOF systems have been performed, employing different input ground motions.

## **2. DEFINITION OF THE SDOF SYSTEM EQUIVALENT TO THE MACROELEMENT AND OF THE NON-LINEAR ELASTIC FORCE-DISPLACEMENT (ROTATION) RELATIONSHIP**

The dynamic behaviour of a macroelement belonging to a monumental building, develops as the loss of equilibrium of rigid blocks capable of sliding and rotating when the masonry shows good characteristics (regular texture, transversal connection between the masonry leaves). In the framework of a displacement-based approach, the representation of the dynamic response of a macroelement in terms of an equivalent single-degree-of-freedom (SDOF) oscillator makes reference to a plausible kinematic configuration, rather than to the deflection shape of the fundamental mode of vibration, as in the case of multi-storey buildings.

The identification of a plausible kinematism (a kinematic configuration) is obtained by positioning a sufficient number of hinges or sliding planes, and identifying the dead loads and the horizontal seismic actions for each resulting block. As an example, the typical collapse mechanisms of a façade and of a triumphal arch in a church are shown in Figs. 1-a and 1-b.

The modal participation factor  $\Gamma$  and the modal mass coefficient  $m^*$  are evaluated making reference to the vector of the virtual horizontal displacements  $\delta_x$ , representing the mode of failure, as in Annex 11.C (OPCM 3431/2005).

The non-linear elastic force-displacement (rotation) relationship is defined applying an incremental kinematic approach, based on the equilibrium limit analysis. Each block of the assumed kinematism is subjected to dead loads and to horizontal seismic action, proportional to the dead loads through a coefficient  $\alpha$ . Under the hypothesis of non-tensile strength of masonry, unlimited compressive strength and rigid blocks, the seismic coefficient  $\alpha_0$  that induces the loss of equilibrium is obtained by the principle of virtual works (Annex 11.C OPCM 3431/2005).

By applying an infinitesimal variation to the equilibrium configuration, i.e. an infinitesimal rotation  $\theta_k$  or displacement  $d_k$  to the  $k$ -th block of the assumed kinematism, the current displacement state of the blocks is obtained by the kinematic theorem, and the same is for the displacements of each relevant point. The incremental analysis must be performed till to the zeroing of the coefficient  $\alpha$ , that occurs for a displacement  $d_{k,0}$ ; if the different actions may be considered as constant during the progression of the kinematism, the resulting non-linear elastic force-displacement (rotation) relationship may be well approximated by a straight line (Annex 11.C OPCM 3431/2005).

The curve obtained through the incremental kinematic analysis is then transformed into the equivalent single degree of freedom capacity curve (Fig. 1-c, positive-axis values) via the equivalent mass modal mass coefficient  $m^*$  and the modal participation factor  $\Gamma$  previously introduced. On the one hand, the horizontal spectral acceleration  $a_0$  that activates the mechanism (representing the capacity in terms of strength) is obtained from the seismic coefficient  $\alpha_0$ . On the other hand, the horizontal spectral displacement  $d_0$ , representing the ultimate displacement, is computed from displacement  $d_{k,0}$  corresponding to the zeroing of the coefficient  $\alpha$ . In Annex 11.C (OPCM 3431/2005), the capacity in terms of displacement (for the ultimate limit state) is given by  $0.4 d_0$ . Analyses from real study cases (Giovinazzi *et al.* 2006) have lead to the selection of suitable range of capacity properties in terms of acceleration  $a_0$  and displacement  $d_0$  for SDOF systems representative of church façades. A total number of 864 equivalent SDOF systems were in the end considered assuming parametric values of  $a_0$ ,  $d_0$  and  $T_0$  (initial period ranging from 0.1 s to 0.6 s).

### 3. THE DYNAMIC RESPONSE OF THE SDOF NON-LINEAR SYSTEM EQUIVALENT TO THE STRUCTURE

#### 3.1 Definition of the procedure to assess the dynamic response of the SDOF non-linear system

The adopted model for the description of the equivalent SDOF motion, is similar to Housner's one (Housner 1963), introducing the initial elastic branch representing the overall stiffness (Fig. 1-c). The Housner's non-linear oscillator is characterised by elastic behaviour, with softening range, where the energy dissipation in the rocking response of rigid blocks (mainly originates from the impact associated with the closing of cracks) is translated into an equivalent viscous damping coefficient and accounted for in the reaction force assessment.

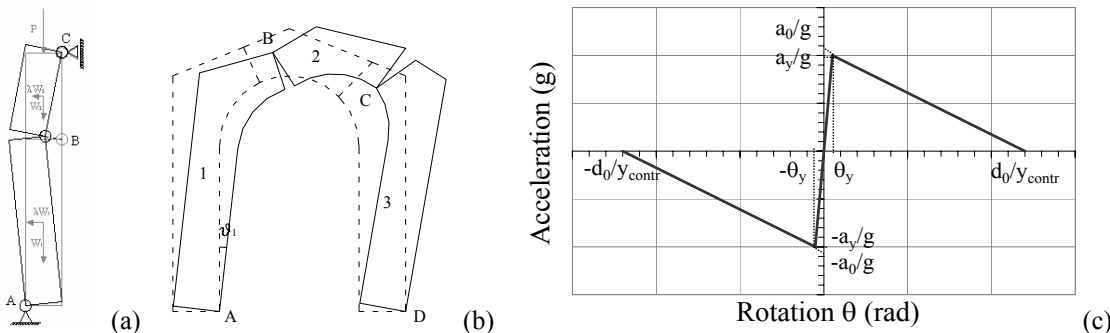


**Figure 1: Typical kinematisms for different macroelements: a) two blocks kinematism for a church façade (in presence of a constraint due to a longitudinal tie-rod in the upper part), b) three blocks kinematism for a triumphal arch. c) Bi-linear capacity curve with ascending branch, in terms of acceleration (unit of g) and rotation, representing the reaction force  $r(\theta)$ .**

The procedure involves the modification of the equations of motion, in particular of the reaction force  $r(\theta)$ , function of the rotation  $\theta$ , substituting the relation of the capacity curve obtained by non-linear kinematic method. The cyclic behaviour does not allow hysteretic dissipation, but, being non-linear elastic, the value of the

equivalent viscous damping (beyond the initial range) may be related to the rotation  $\theta$ , through the secant period  $T$  corresponding to  $\theta$ .

For damped forced vibrations, the equation of motion for the non-linear oscillator is:

$$\ddot{\theta} + \gamma \dot{\theta} + p^2 r(\theta) = -p^2 \frac{a_g(t)}{g} \quad (1)$$

where  $\theta = \theta(t)$  is the rotational degree of freedom and  $\dot{\theta}$  and  $\ddot{\theta}$  are, respectively, its first and second time derivative,  $\gamma$  is the damping coefficient defined as a function of the equivalent viscous damping  $\xi_{eq}$  (see § 4),  $r(\theta)$  is the reaction force function,  $a_g(t)$  is the ground acceleration ( $m/s^2$ ),  $g$  is the gravity acceleration ( $m/s^2$ ).

The coefficient  $p^2$  is evaluated for undamped free vibration resulting in:

$$p^2 = \frac{1}{\omega_0^2} \frac{g}{a_y} \theta_y = \frac{4\pi^2}{T_0^2} \frac{g}{a_y} \theta_y = \frac{g}{y_{contr}} \quad (2)$$

where  $T_0$  and  $\omega_0$  are respectively the initial period and the initial frequency evaluated for the initial ascending branch,  $\theta_y$  is the maximum rotation for the initial ascending branch,  $a_y$  is the acceleration on the curve of the SDOF system when  $\theta = \theta_y$ ,  $y_{contr}$  is the height of the control point.

An ad hoc numerical program has been implemented in order to obtain the numerical solution of the dynamic motion for the non-linear oscillator. The explicit method proposed by Runge-Kutta (Forsythe *et al.* 1977) has been assumed for the numerical integration of the equation of motion.

### 3.2 Accelerometric database

A selected set of high quality digital strong motion data from different regions (Italy, California, Japan, Iran, Island, Mexico, Turkey) has been employed for the analyses, provided by the research group of Milan Polytechnic. This database is part of a dataset currently employed for the improvement of the formulation of the displacement response spectra over a wider period range (Project S5 ProCiv-INGV, 2004-2006). The digital strong motions have been recorded on different soil conditions, have a different duration and a magnitude in the range from 5.5 to 7.2 (Table 1). All the records have been baseline corrected.

**Table 1: The accelerometric database used for the dynamic analyses.**

Name	Earthquake event	Year	$M_w$	Station	$R_{closest}$ (km)	Soil (EC8)	PGD (m)	PGA ( $m/s^2$ )	$t(s)^*$
EQ1	Umbria-Marche - Italy	1997	5.5	Colfiorito Casermette	5	A	0.01	2.27	20.0
EQ2	Umbria-Marche - Italy	1997	5.5	Nocera Umbra Biscontini	10	A	0.02	4.43	25.6
EQ3	Umbria-Marche - Italy	1997	6.0	Gubbio Piana	38	C	0.05	1.13	106.2
EQ4	California - Parkfield	2004	6.0	Jack Canyon	19.2	-	0.01	1.44	103.7
EQ5	California - Parkfield	2004	6.0	Eades	9.8	-	0.05	3.87	40.0
EQ6	Japan	2005	6.1	CHB010	5	C	0.06	2.84	54.0
EQ7	Japan	1997	6.3	KGS002	12	B	0.05	5.98	40.0
EQ8	Iran - Bam	2003	6.5	Bam	0	C	0.35	7.88	66.5
EQ9	Island	2000	6.5	Hella	15	B	0.15	4.64	81.0
EQ10	Mexico	2000	7.0	Caleta de Campos	15.1	A	0.02	1.10	89.0
EQ11	Japan - Kobe	1995	7.2	Port Island Borehole	17.4	C	0.32	2.83	120.0
EQ12	Turkey - Duzce1	1999	7.2	Bolu-Bayindirlik	39	C	0.37	7.34	55.9

\*effective duration based on the Arias' intensity.

Statistically independent artificial acceleration time histories of different duration (15s and 20s) have been generated (SIMQKE, Gasparini and Vanmarke 1976) matching EC8 design response spectra; reference has been made to  $a_g = 0.35g$  design ground acceleration for soil classes A, B and D.

## 4. EVALUATION OF THE DAMPING RELATIONS

Three different relationships are proposed in this paper for the definition of the equivalent viscous damping ratio  $\xi_{eq}$ , as a function of the rotation  $\theta$  (which the secant period  $T$  corresponds to).

The initial viscous damping ratio  $\xi_0$  has been defined on the basis of the initial period  $T_0$ , being equal to a

reference value  $\xi_i=5\%$  if the initial period  $T_0$  is smaller then an assumed conventional period  $T_1$  (a value  $T_1=0.4$  s is proposed for  $T_1$ ), evaluated in such a way to keep constant the damping coefficient  $\gamma$  otherwise:

$$\begin{cases} \xi_0 = \xi_i & \text{if } \omega_0 \geq \omega_i \ (T_0 \leq T_1) \\ \xi_0 = \xi_i \frac{\omega_i}{\omega_0} & \text{if } \omega_0 < \omega_i \ (T_0 > T_1) \end{cases} \quad (3)$$

where  $T_0$ ,  $\omega_0$ ,  $\xi_0$  are respectively the fundamental period, frequency and viscous damping ratio evaluated for the initial ascending branch and  $\omega_i$  and  $\xi_i$  are the frequency and viscous damping ratio related to  $T=T_1$ .

Figure 2 shows the representation of the proposed formulations for the equivalent viscous damping as a function of the period  $T$ , for the two cases  $T_0 < T_1=0.4$  s,  $T_0 > T_1=0.4$  s.

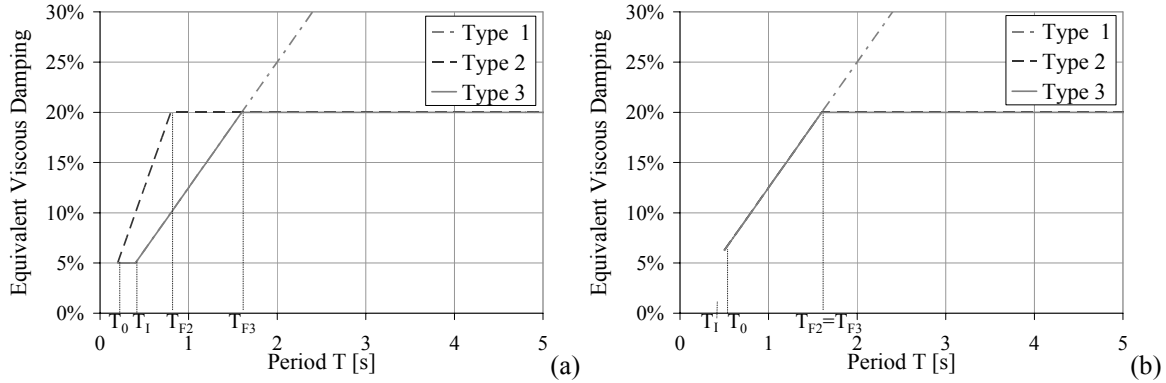


**Figure 2: Proposals for the different definition of the equivalent viscous damping depending on the initial period: a)  $T_0 < T_1=0.4$  s, b)  $T_0 > T_1=0.4$  s.**

A first proposal for the assessment of the equivalent viscous damping (Type1) concerns a constant value ( $\xi_{eq}=5\%$ ) for  $T \leq T_1$  and an ascending branch (proportional to  $T/T_1$ ) for  $T > T_1$ .

The second proposal (Type2) for the definition of the equivalent viscous damping accounts for a superior limit for  $\xi_{eq}$  in the non-linear phase. A value of  $\xi_F=20\%$  has been assumed for the equivalent final viscous damping  $\xi_F$  when  $T=T_F$ . A constant damping coefficient  $\gamma$  for the period values  $T_0 \leq T < T_F$ , corresponding to a linear variation of the equivalent viscous damping with period, is also established.

A third proposal for the equivalent viscous damping (Type3) is formulated in order to account for both the constant value ( $\xi_{eq}=5\%$ ) for  $T \leq T_1$  and for the superior limit for the equivalent viscous damping  $\xi_F$  in the non-linear phase for  $T \geq T_F$ . A linear variation of the equivalent viscous damping with period for  $T_1 \leq T < T_F$ , is defined.

First of all, the constant value ( $\xi_{eq}=5\%$ ) for  $T \leq T_1$  has been suggested in such a way to make the non-linear phase close to the ascending branch as much independent as possible from the assumed initial vibration period  $T_0$ . This has been proposed in order to analyze the possibility of obtaining results, in terms of maximum rotation or displacement, less affected by the assigned  $T_0$ . As previously highlighted, the initial dynamic behaviour of a macroelement, part of a monumental masonry building, is related both to the element stiffness and to the structure stiffness, because of their interaction. The estimate of vibration period  $T_0$  associated to the mechanism in the phase preceding its activation is therefore difficult and it is affected by a great amount of uncertainty.

Secondly, the assumption of a superior limit for the equivalent viscous damping in the non-linear phase is justified from experimental studies on rocking systems (Doherty *et al.* 2002) that have shown how for high period values, the damping ratio is lower than 20%.

These three damping relations have been implemented in the numerical program where the reaction force  $r(\theta)$  is evaluated step by step in the equation of motion for  $\theta=\theta(t)$ , according to the different laws.

## 5. THE SIMPLIFIED PROCEDURE TO EVALUATE THE DYNAMIC RESPONSE

The proposed non-linear kinematic simplified approach for macroelements belonging to monumental structures, introduces overdamped elastic spectra for the evaluation of the maximum response in terms of displacement (or rotation  $\theta$ ).

The use of overdamped spectra allows us to account for the influence of the equivalent viscous damping (on the maximum response of the structures in terms of displacement), that strongly increases when the initial phase is

overcome, as clearly shown from experimental evidences about rocking elements (Doherty *et al.* 2002). For the 864 equivalent SDOF systems, the performance-point assessment resulting applying the proposed procedure has been compared with the results obtained from the dynamic analyses (in terms of displacement). The equivalent viscous damping ratio  $\xi_{eq}$  to be adopted for the response spectra reduction has been evaluated in correspondence of the maximum rotation  $\theta_{max}$  obtained by the dynamic analyses.

For this purpose, for each of the SDOF systems considered for the dynamic analysis, the secant period corresponding to the resulting maximum rotation  $\theta_{max}$  has been firstly assessed  $T_{max}=T(\theta_{max})$ . The equivalent viscous damping ratio  $\xi_{eq}=\xi_{eq}(T_{max})$ , corresponding to that period, has been evaluated according to the correlations proposed for  $\xi_{eq}$  in § 4. The factor for the elastic spectrum reduction has been computed according to the formula proposed by EC8 (eq. 3.6 in §3.2.2.2) as a function of the assessed  $\xi_{eq}$ . The obtained value for  $T_{max}$  on the overdamped spectra (reduced as a function of  $\xi_{eq}=\xi_{eq}(T_{max})$ ) has provided the expected displacement response  $S_d(T_{max})$ , and the related acceleration  $S_a(T_{max})$ , according to the proposed non-linear simplified procedure.

For the validation of the results obtained via the non-linear kinematic approach in terms of  $S_d(T_{max})$  and  $S_a(T_{max})$ , the correspondence with the output from the dynamic analysis in terms of displacement  $d_{max}$  (corresponding to  $\theta_{max}$ ) and acceleration  $a(T_{max})$  has been checked as explained in the following.

## 6. VALIDATION OF THE SIMPLIFIED PROCEDURE THROUGH THE DYNAMIC ANALYSIS

For the validation of the simplified procedure, reference is made to a particular kind of result representation. In Fig. 3, an example is proposed; Fig. 3-a, in ADRS format, shows:

- the elastic spectrum (damping ratio 5%);
- the capacity curves of two SDOF systems (SDOF1 and SDOF2), where the last point represents the value of  $d_{max}$  and the corresponding  $a(T_{max})$  obtained by the dynamic analyses (representing the benchmark for these results).
- the overdamped spectra, for the two cases, where the reduction factor is related to the value of  $\xi_{eq} = \xi_{eq}(T_{max})$ .

In the case of SDOF1, the simplified procedure matches with the dynamic result (in a few words, the value of the equivalent viscous damping  $\xi_{eq}(T_{max})$  corresponds to the correct spectral reduction). In the case of SDOF2, the simplified procedure does not provide a correct estimation. It is worth noting that the data in Fig. 3 do not allow us to quantify the error between the dynamic and the simplified method, standing that (without knowing the dynamic result) the simplified procedure imposes to iterate, changing the secant period  $T$ , until the intersection of the capacity curve and the overdamped spectrum ensures the correspondence of the computed value of  $\xi_{eq} = \xi_{eq}(T)$ . This feature is analysed later (§ 6.1).

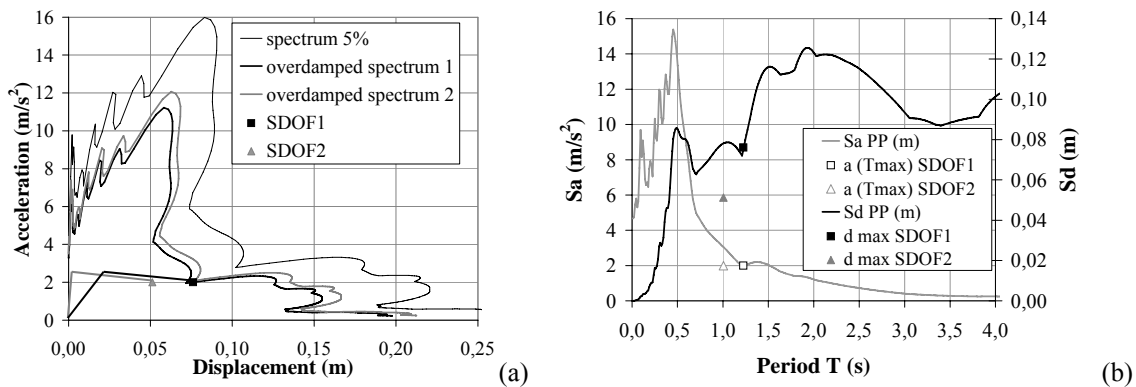


**Figure 3: Comparison between dynamic analysis and simplified procedure: (a) example in ADRS format; (b) example inserting an ordinate secondary axis.**

In Fig. 3-b, the same results are shown, inserting an ordinate secondary axis. The following quantities are represented:

- the displacement spectrum  $S_d$  vs. the period  $T$ ;  $S_d$  is reduced by a factor function of the period, depending on  $\xi_{eq}(T)$ ;
- the acceleration spectrum  $S_a$  vs. the period  $T$ ;  $S_a$  is reduced by a factor function of the period, depending on  $\xi_{eq}(T)$ ;
- the maximum displacement  $d_{max}$  resulting from the dynamic analysis vs. the period  $T$ ;
- the acceleration  $a(T_{max})$  corresponding to the maximum displacement  $d_{max}$  vs. the period  $T$ .

The simplified procedure matches with the dynamic result when, for the calculated  $T_{\max}$  value,  $d_{\max}$  lays on the overdamped displacement spectrum  $S_d$  and, contemporaneously,  $a(T_{\max})$  lays on the overdamped acceleration spectrum  $S_a$  (as in case of SDOF1).

## 6.1 Validation employing artificial acceleration time histories

The first phase for the validation of the simplified procedure is based on the result comparison using 18 artificial acceleration time histories of different duration (15s and 20s) matching EC8 design response spectra ( $a_g=0.35g$ , soil type A, B and D). For each one of the 864 equivalent SDOF systems considered (having  $0.1 \leq T_0 \leq 0.6$  s and  $0.2 \text{ m/s}^2 \leq a_0 \leq 3.2 \text{ m/s}^2$ ;  $0.5 \text{ m} \leq d_0 \leq 2.1$  m - soil A;  $0.5 \text{ m/s}^2 \leq a_0 \leq 8 \text{ m/s}^2$ ;  $0.5 \text{ m} \leq d_0 \leq 2.1$  m - soil B;  $0.8 \text{ m/s}^2 \leq a_0 \leq 12.8 \text{ m/s}^2$ ;  $0.7 \text{ m} \leq d_0 \leq 2.3$  m - soil D), the dynamic analyses are implemented and the displacement demand (performance-point assessment) resulting applying the proposed simplified procedure has been compared with these results.

The damping relationships to be adopted for the equivalent viscous damping ratio  $\xi_{eq}$  are the ones previously mentioned Type1, Type2 and Type3.

In Fig. 4, employing the result representation in Fig. 3-b, some results are proposed (time history 1, 20s, for soil A and time history 1, 20s, for soil D), using the EC8 response spectrum format, adequately reduced in order to consider the overdamping effect.

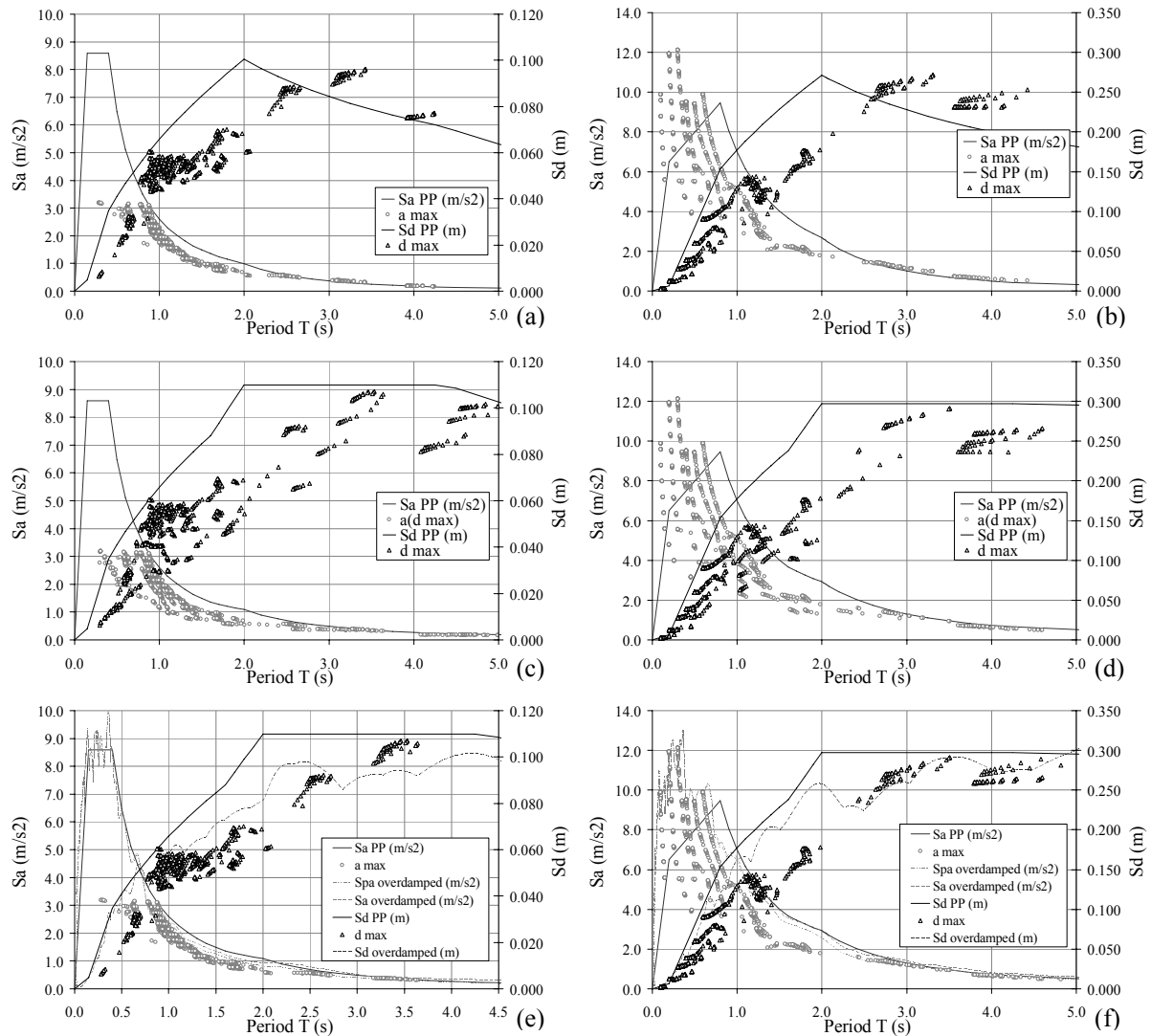


**Figure 4: Comparison between dynamic analysis and simplified procedure: soil A, damping relation (a) Type1; (c) Type2; (e) Type3; soil D, damping relation (b) Type1; (d) Type2; (f) Type3.**

It can be noted that, in case of Type1 damping relation, the non-linear kinematic procedure underestimates the response in the long-period range (not ensuring a safe estimation). This is clearly ascribable to the unbounded

increase of damping ratio  $\xi_{eq}$ , more influencing the simplified method, in which the response depends only on  $\xi_{eq}(T_{max})$ , while in the dynamic analyses the non-linear behaviour also involves a larger frequency range. If Type2 damping relationship is employed, the response scattering in the medium-large period range considerably increases. In fact, with this kind of law the response is strongly influenced by the choice of the initial period  $T_0$ .

On the other hand, if Type3 damping relationship is considered, the dynamic response is affected by some scattering only in the low period range, less interesting in this study. In particular, if the real response spectra of the used time history, dotted lines in Figs. 4-e and 4-f, (obviously not perfectly matching the target EC8 spectra) are accounted for, in the medium-large period range, the forecasting obtained by the simplified procedure is wholly matching the dynamic results. This is a further confirmation that the imposition of an upper bound for the equivalent viscous damping ratio should be highly recommended for this kind of procedures.

Analysing Type3 damping relation, interesting results can be shown in terms of maximum displacement from dynamic analyses (namely  $d_{max}$ ) and performance-point displacement  $S_d(T_{pp})$  obtained by the simplified method, employing the typical iterative procedure. In this case, the secant period  $T_{pp}$  is modified, until the intersection of the capacity curve and the overdamped spectrum ensures the correspondence of the computed value of  $\xi_{eq} = \xi_{eq}(T_{pp})$ . Obviously the  $T_{pp}$  value is equal to  $T_{max}$  only if, in Fig. 4, the overdamped displacement spectrum  $S_d$  perfectly matches with the representative point resulting from the dynamic analysis.

In Fig. 5-a, non negligible scatter can be noticed between the displacement estimation for the 864 SDOF systems (time history 1 - 20s - soil A), but, if the attention is focused on medium-large period range (1.0÷6.0 s) and particularly on large period range (2.5÷6.0 s), the displacement ratio is reasonably near to 1 (Fig. 5-b).

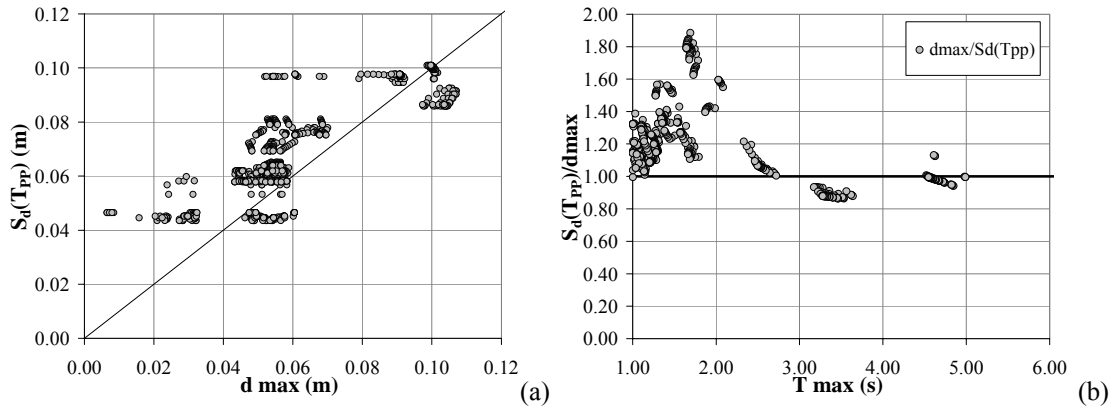


**Figure 5: (a) Maximum displacement from dynamic analyses vs. PP displacement (iterative procedure); (b) Displacement ratio vs. secant period  $T_{max}$  (soil A, Type3 damping relation).**

Similar outcomes may be achieved in case of the other time histories: as an example, the results for time history 1 - 15s - soil B and time history 1 - 20s - soil D are shown in Fig. 6.

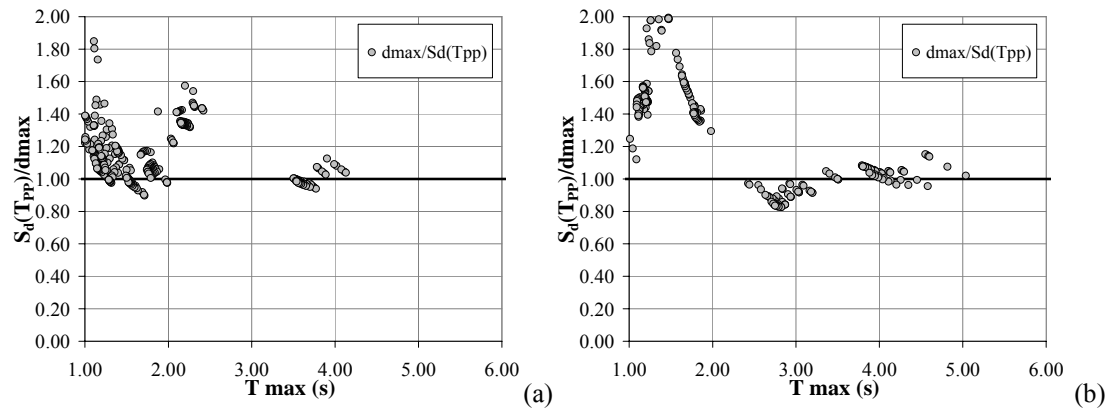


**Figure 6: Displacement ratio vs. secant period  $T_{max}$  (Type3 damping relation): (a) soil B; (b) soil D.**

## 6.2 Validation employing the recorded accelerometric database

The following phase for the validation of the simplified procedure is based on the result comparison using the recorded time-history database provided by the research group of Milan Polytechnic (Table 1). For each of the 864 equivalent SDOF systems considered (having  $0.1 \text{ s} \leq T_0 \leq 0.6 \text{ s}$  and  $0.1 \text{ m/s}^2 \leq a_0 \leq 8 \text{ m/s}^2$ ;  $0.5 \text{ m} \leq d_0 \leq 2.1 \text{ m}$ ), the



dynamic analyses are implemented, applying the previously proposed procedure for the result comparison. The damping laws for the equivalent viscous damping ratio  $\xi_{eq}$  to be adopted are the before mentioned Type1, Type2 and Type3. Having verified that the influence of the damping definition is the one previously described, some results are proposed in Fig. 7 (EQ 1 - Umbria-Marche; EQ 12 - Turchia - Duzcel), employing Type3 damping relationship and the result representation in Fig. 3-b.

It is worth noting that, in Fig. 7, two kind of spectra are shown: the elastic spectrum reduced in order to consider the overdamping effect using the EC8 factor (continuous line) and the response spectrum derived by the maximum response of linear SDOF systems, for which the damping ratio (related to vibration period  $T$ ) is computed on the basis of Type3 relation (dotted line). The dynamic response of the SDOF systems is evaluated in the time domain through a convolution integral.

Moreover, it can be highlighted, as described later (§ 6.3), that for very high values of damping ratio (corresponding to the large period range), the spectral reduction factor proposed by EC8 underestimates the displacement demand, in case of many recorded time histories.

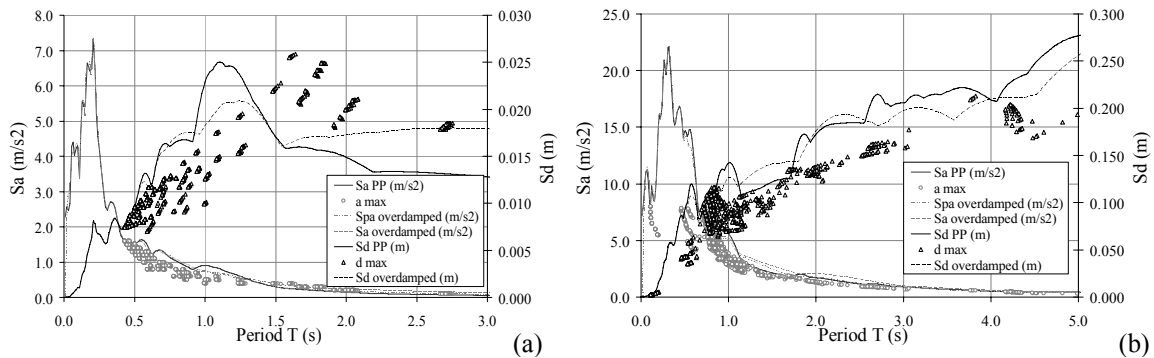


**Figure 7: Comparison between dynamic analysis and simplified procedure: Type3 damping relation (a) EQ 1 - Umbria-Marche; (b) EQ 12 - Turkey-Duzcel.**

Making reference to EQ 1 - Umbria-Marche (Fig. 7-a) or EQ 5 - California-Parkfield, some troubles may be pointed out applying the simplified procedure. In fact, if the displacement spectrum is characterised by high-harmonic content in the period range near  $T_{max}$ , but  $S_d(T_{max})$  is lower, the computed displacement value in the simplified method underestimates the dynamic value. In fact, in the simplified method, the response depends only on  $\xi_{eq}(T_{max})$ , while in the dynamic analyses the non-linear behaviour also involves a larger frequency range. The opposite trend is also noticed. At now, no correlation between the seismic input characteristics (Arias' intensity, magnitude, etc.) and the dynamic results has been found by the authors. If the spectra do not show remarkable alternate peaks and gaps (for the different period ranges), as EQ 12 - Turkey-Duzcel (or EQ 7 - Japan), the simplified method provides quite good results (mainly on the safe side), as in Fig. 7-b.

### 6.3 Further considerations on spectral reduction factors

The resulting ratio between the damped spectral ordinates applying different scaling factors and the damped spectral ordinates derived by the maximum response of linear SDOF systems (in the time domain through a convolution integral) has been investigated. Different spectral reduction factors have been considered from a review of Bommer and Mendis (2005).

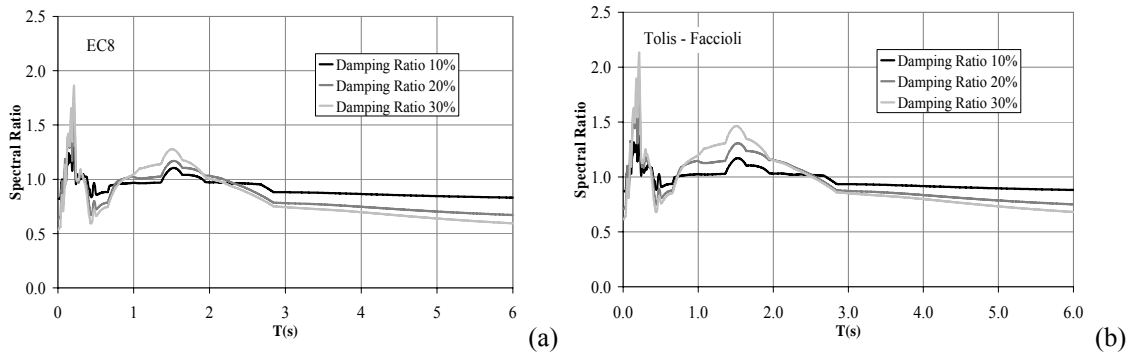


**Figure 8: Spectral ratio between the damped spectral ordinates. Scaling factor from: a) EC8 (Bommer et al., 2000), b) Tolis and Faccioli 1999.**

In particular, Fig.8 shows these ratios as a function of the period with reference to Bam earthquake (EQ8 in Table 1), in case of two spectral reduction factors. For all the scaling factors applied, the underestimation of the damped spectral ordinates is observed for high period values. The underestimation increases for higher damping ratio. The same trend has been observed for the majority of the earthquake in the dataset (Table 1).

The reduction factor proposed in the framework EC8 (Bommer *et al.*, 2000) has been employed for the analyses presented in this paper. A proposal for a reduction factor more suitable for the representation of the high period range is expected as a result of a research project in progress (Project S5 ProCiv-INGV, 2004-2006).

## 7. CONCLUSIONS AND FURTHER DEVELOPMENTS

The main objective of the proposed study has been, first of all, the validation (in the large period range) of the displacement-based approach through non-linear kinematic analysis for monumental buildings. An important outcome is represented by the correspondence between the non-linear time-history analysis results and the simplified predictions through overdamped elastic spectra (employing the artificial acceleration database), if the damping relation is almost independent from the initial period  $T_0$  and an adequate upper bound is considered.

Moreover, the troubles related to the recorded accelerometric database have to be carefully investigated in order to assess the reliability and the feasibility of the proposed approach, even if, at now, no correlation between the seismic input characteristics (Arias' intensity, magnitude, etc.) and the dynamic results has been found.

In order to overcome the discrepancies in the estimated displacement value, a term or a sub-procedure accounting for the harmonic content in the period range near  $T_{max}$  could be introduced in the simplified method. Further investigations may involve the effect on the SDOF system response of the input duration and the number of cycles in non-linear phase. As a further validation of the proposed model, the implementation for the analysis of case studies, e.g. churches located in the area of Umbria-Marche and Lunigiana-Garfagnana (Italy) for which detailed damage and technological survey are available, is in progress.

## 8. REFERENCES

- Forsythe, G.E., Malcolm, M.A., Moler, C.B. (1977). *Computer Methods for Mathematical Computations*. Englewood Cliffs, NJ: Prentice-Hall.
- Bommer, J.J., Elnashai, A.S., Weir, A.G. (2000). Compatible acceleration and displacement spectra for seismic design codes. *Proc. of the 12th WCEE*, Auckland. Paper no 207.
- Bommer, J.J., Mendis R. (2005). Scaling of spectral displacement ordinates with damping ratios. *Earthquake Engineering and Structural Dynamics*, 34:145–165.
- Dogliani, F., Moretti, A. & Petrini, V. (1994). *Le chiese e il terremoto*. Trieste: Edizioni LINT (in Italian).
- Doherty, K.T., Griffith, M.C., Lam, N., Wilson, J. (2002). Displacement-based seismic analysis for out-of-plane bending of unreinforced masonry walls. *Earth. Eng. and Struct. Dyn.*, 2002;31(4). pp. 833–50.
- Fajfar, P. (2000). A nonlinear analysis method for performance-based seismic design. *Earth. Spectra*, 16(3): 573-592.
- Gasparini, D. and Vanmarke E. H. (1976), *Simulated Earthquake Motions Compatible with Prescribed Response Spectra*, M.I.T., Department of Civil Engineering Research Report R76-4, Order No. 527.
- Giovinazzi, S., Lagomarsino, S., Resemini, S. (2006). Displacement capacity of ancient structures through non-linear kinematic and dynamic analyses. *Proc. of SAHC 2006*, New Delhi 2006 (in press).
- Heyman, J. (1966). The stone skeleton, *International Journal of Solids and Structures*, 2, pp. 249-279.
- Housner, G.W. (1963). The behaviour of inverted pendulum structures during earthquakes, *Bullettin of the Seismological Society of America*, 17, pp.40-417.
- Lagomarsino, S. (2005). Chapter7. Vulnerability assessment of historical buildings. In *Assessing and Managing Earthquake Risk - Geo-scientific and Engineering Knowledge for Earthquake Risk Mitigation: developments, tools, techniques*. Series: Geotechnical, Geological, and Earthquake Engineering, 2. Oliveira, Carlos Sousa; Roca, Antoni; Goula, Xavier (Eds.). ISBN: 1-4020-3524-1.
- Lam, N., Nurtug, A., Wilson, J. (1998). Shaking Table Testing of Parapet Walls with Periodic and Transient Excitations, University of Melbourne, Dept. Rep. No. RR/STRUCT/98.
- OPCM, no. 3431, 3 May 2005. Official Bulletin no. 107, 10 May 2005 (in Italian).
- Paolucci R., Faccioli E., García-Mayordomo J. (2004), Displacement response spectra at long periods: an application to seismic hazard assessment in Southern Italy, *Proc. of the 13<sup>th</sup> World Conf. on Earth.Eng.*, Paper 1969.
- Project S5 – Seismic input definition on the basis of expected displacements*. Coordinators E. Faccioli and A. Rovelli, ProCiv-INGV, 2004-2006.
- Tolis, S.V., Faccioli, E. (1999). Displacement design spectra. *Journal of Earthquake Engineering*, 3(1):107–125.